Crop Sci. Accepted Paper, posted 02/15/2019. doi:10.2135/cropsci2018.10.0609

Analysis and modelling of processes involved with salt tolerance and rice

Sofia Tartarini[1,*], Livia Paleari[1,*], Ermes Movedi[1], Gian Attilio Sacchi[2], Fabio Francesco Nocito[2], Roberto Confalonieri[1]

[1]: Università degli Studi di Milano, ESP, Cassandra lab, via Celoria 2, 20133 Milan, Italy

[2]: Università degli Studi di Milano, DISAA, via Celoria 2, 20133 Milan, Italy

* Corresponding authors: sofia.tartarini@unimi.it (S. Tartarini), livia.paleari@unimi.it (L. Paleari)

Abbreviations: AGB, above ground biomass; CRM, coefficient of residual mass; DVS, Development stage; EF modelling efficiency; G × E × M, genotype × environment × management interaction; gLAI, Green Leaf Area Index; MAE, mean absolute error; SLA, Specific Leaf Area.

Keywords: breeding programs, *Oryza sativa* L., salinity stress, salt tolerance, trait-based model.

Highlights:

- We evaluated a trait-based model for the ionic component of salt stress
- Large variability in the effect of salt stress was observed among rice cultivars
- Different physiological mechanisms were involved in response to salinity
- The model successfully reproduced Na^+ dynamics and impacts for different genotypes
- Model parameter distributions for ideotyping studies are provided

Abstract

Salinity is a worldwide problem for rice cultivation and a number of breeding programs targeting increased salt tolerance are ongoing. A new trait-based mathematical model for salt stress on rice was recently proposed, characterized by a high level of detail in the description of physiological mechanisms dealing with crop response to salinity. In this study, dedicated growth chamber experiments were carried out where three rice cultivars with different degree of tolerance were grown under different salinity levels. The aims were to improve the understanding of physiological mechanisms like Na^+ uptake and sequestration in structural tissues, and to validate the model using new datasets where temporal dynamics in plant response to salt stress were analyzed. Model evaluation demonstrated a good agreement between measured and simulated dry weights of plant organs (e.g., R^2 ranged from 0.88 to 0.97 for aboveground biomass), $[Na^+]$ in plant tissues (R^2 from 0.73 to 0.88), and green leaf area index (R^2 from 0.71 to 0.99). These results demonstrate the reliability of the model, and support its adoption within studies aimed at analyzing or predicting the response of different cultivars to temporal dynamics of Na^+ concentration in soil and water.

Crop Sci. Accepted Paper, posted 02/15/2019. doi:10.2135/cropsci2018.10.0609

1. Introduction

With almost 160 million ha harvested worldwide (www.faostat.fao.org), rice represents the staple food for more than half of the world's population (IRRI, 2006), influencing the livelihood of more than three billion people and the economy of several countries. World rice production must increase by about 1% per year to meet the growing demand for food that will result from an ever-increasing population (FAO, 2009). Among the main obstacles to increase rice production in many areas worldwide, a key role is played by salinization, being rice the most sensitive cereal to salt-induced stress (Munns and Tester, 2008). The extent of salt-affected soils (more than 830 million hectares, 6% of the world's land; FAO, 2008) led to identify salinization as a major process of land degradation, and the main cause of land desertification in arid or semi-arid regions (Aringhieri, 2010). Ecological, climatic and management conditions can lead salt accretion in top soil to be caused by different factors (Reynolds et al., 2001), ranging from irrigation with saline water in poor draining soils to natural causes (i.e., tsunami, deposition of oceanic salts, saline wedge intrusion).
In case of saline soils, plants have to cope with two major stresses: osmotic and ionic (Horie, 2012). The former rapidly affects plants once salt concentration outside the roots increases, reducing water uptake, cell expansion, and lateral bud development (Munns and Tester, 2008). The ionic stress, instead, occurs later, when toxic ions like Na^+ accumulate in tissues (especially leaves) until exceeding a threshold concentration. In this case, effects are leaf chlorosis and necrosis, a decrease in the activity of essential cellular metabolic processes, including photosynthesis (Glenn et al. 1999), and spikelet sterility (Hossain et al., 2015).
A quantitative understanding of the different mechanisms involved with salt stress would represent a solution for increasing food production (Reddy et al., 2017), given it would allow developing cultivars improved for the specific traits that guarantee the largest benefits for the salinity dynamics affecting a given rice district (Paleari et al., 2017a). However, progresses in dedicated breeding programs were limited by (i) gaps in the knowledge of the genetic basis of tolerance, (ii) the

involvement of different complex tolerance mechanisms, (iii) inadequate screening techniques, and (iv) low selection efficiency (Yeo and Flower, 1986; Reddy et al., 2014).

Ecophysiological models can be used to support breeding programs by means of different strategies to relate model parameters to genotypic and phenotypic plant features (Parent and Tardieu, 2014; Casadebaig et al., 2016; Tao et al., 2017). The combined use of models and mathematical procedures to explore parameter hyperspaces allows evaluating in a quantitative way the traits breeders are working on, in turn allowing the identification of most promising ones under specific agro-climatic and management conditions (Martre et al., 2015) and suggesting optimum values for them (Paleari et al., 2017b). Relationships between model parameters and QTLs (Yin et al., 1999) or SNPs (Cooper et al., 2016) were instead used to predict the performance of genotypes starting from genetic information. Given the relevance of salt stress for agricultural productions, different models reproducing crop response to salt stress were developed (e.g., Ferrer Alegre et al., 1997; Karlberg et al., 2006, Radanielson et al., 2018). However, they mainly focus on the effect of the osmotic stress on water uptake, without explicitly considering the ionic effect of Na^+ which, instead, is a key component of salt stress (Munns and Tester 2008; Faiyue et al., 2012), especially in rice (Negrão et al., 2011). Furthermore, these approaches lack of an explicit representation of morphological and physiological traits in model parameters.

A new model for the simulation of the ionic component of salt stress was recently proposed by Paleari et al. (2017a). The model focuses on the key mechanisms that regulate Na^+ uptake, Na^+ sequestration into different organs and related impact on photosynthesis, leaf senescence, and spikelet sterility. Given it was developed to support breeding activities, it explicitly accounts for genotype-specific traits contributing to salt tolerance.

Na^+ uptake at root level is reproduced considering both apoplastic (bypass flow) and symplastic pathways. Bypass flow-Na^+ uptake, one of the key factors which may determine genotypic differences for salt tolerance in rice (Faiyue et al., 2012), is driven by plant transpiration, by the fraction of water passing through the apoplast, and by the development of Casparian bands and

Crop Sci. Accepted Paper, posted 02/15/2019. doi:10.2135/cropsci2018.10.0609

suberin lamellae in root tissues which reduce water movement through the apoplast. Root suberin content is estimated according to plant age and to the genotype-specific efficiency in root suberin deposition as response to salinity in the soil medium. To cope with the Na^+ entering the xylematic stream and translocated to the shoot, rice developed tolerance mechanisms aimed at preventing toxic ions from reaching photosynthetically active tissues. They involve sequestration of Na^+ in structural tissues (culm base and leaf sheath), and in senescent leaves. In the model, the former is reproduced by accounting for genotype-specific culm storage potential and for feedback mechanisms driven by the Na^+ already accumulated in culms, whereas the latter is estimated considering the genotype-specific potential to sequester Na^+ in leaves of different age. A fraction of the Na^+ uptaken to the shoot also reaches panicles, driven by translocation of photosynthates. The reduction of pollen viability driven by the increase in Na^+ concentration in the panicles is estimated by considering the genotypic sensitivity to salt-induced sterility. The negative impact of Na^+ on photosynthetic rate and leaf senescence is derived as a function of Na^+ concentration in the leaf and of the capability of the genotype to sequestrate toxic ions in the vacuole and to counterbalance the osmotic pressure via the synthesis of cytosol-compatible osmolytes. This strategy is often observed in tolerant rice genotypes, since it allows the plant to withstand higher leaf Na^+ concentration (Jacoby et al., 2011).

This study aimed at (i) collecting specific datasets (from growth chamber experiments) to investigate at plant organ level the effects of the ionic component of salt stress, and (ii) parameterizing and evaluating the salinity model developed by Paleari et al. (2017a) for three cultivars differing for salt tolerance.

2. Materials and methods

2.1. Experimental data

Data were collected in two growth chamber experiments, with different rice cultivars grown in hydroponic solutions under different NaCl concentrations. For each cultivar, 180 caryopses were sterilized with 50% (v/v) $Ca(ClO)_2$ for 30 min, thoroughly rinsed with deionized water and placed on wet filter paper at 26°C in the dark for four days. Seven days old seedlings were then transferred to 42 cm × 30 cm × 25 cm (the latter is the height) plastic pots containing the following nutrient solution (Nocito et al., 2011): 1.5 mM KNO_3, 1 mM $Ca(NO_3)_2$, 500 µM $MgSO_4$, 250 µM $NH_4H_2PO_4$, 25 µM $C_4H_4FeO_6$, 46 µM H_3BO_3, 9 µM $MnCl_2$, 0.8 µM $ZnSO_4$, 0.3 µM $CuSO_4$, 0.1 µM $(NH_4)_6MO_7O_{24}$, and 30 µM Na_2O_3Si (pH 6.5). One pot was used for each combination cultivar × treatment, each containing 25 plants. The number of transplanted plants was larger than the foreseen sampling requirements to allow different sampling events without altering too much the plant density in the pots. Polystyrene foam sheets were used to hold seedlings and to allow renewing the hydroponic solutions without touching the plants to avoid any potential damage to the roots (which could cause Na^+ entering directly from root lesions). Nutrient solutions were renewed every three days. Growing conditions were: 14 h photoperiod, 26°C/18°C day/night temperature for the first experiment, and 12 h photoperiod, 26°C/19°C day/night temperature for the second.
Photosynthetically active radiation (400 umol m^{-2} s^{-1}) was supplied by fluorescent lamps.
In the first experiment, two Italian cultivars, Baldo and Vialone Nano (sensitive and highly sensitive to salt stress, respectively; Formentin et al., 2018, Bertazzini et al., 2018), were grown. Five NaCl treatments were applied starting from three weeks after sowing until maturity: 0, 10, 25, 35, and 50 mM. Three plants for each combination cultivar × treatment were harvested at late heading (BBCH code 51; Lancashire et al., 1991) and maturity (BBCH 92), and divided into stems, panicles and leaves. The latter were further separated into apical (the two youngest), mid-canopy, and basal (senescent) leaves to detect potential changes in Na^+ distribution among leaves of different ages. Plant

Crop Sci. Accepted Paper, posted 02/15/2019. doi:10.2135/cropsci2018.10.0609

height, number of tillers and the dry weight of aboveground biomass (AGB; t ha^{-1}) and of biomass of different organs were determined. Grounded dry biomass samples (500 mg) were digested with HNO_3 (10 ml) in a microwave digester at 100°C (Amari et al., 2014). The mineralized material was dissolved in 5 mL of 0.1 M HNO_3, and Na^+ content was measured by inductively coupled plasma mass spectrometry. Immediately before the first sampling event, photosynthetic rate, stomatal conductance and transpiration rate were measured on the youngest fully expanded leaf using a CIRAS-3 Portable Photosynthesis System (PP Systems, MA, USA). Apical and mid-canopy leaves were then digitalized to determine green leaf area index (gLAI, -) and specific leaf area (SLA, m^2 kg^{-1}), the latter calculated as leaf area to dry mass ratio. At harvest, spikelet sterility was determined.

In the second experiment, cultivars Baldo and Pokkali were grown, the latter being considered one of the most salt-tolerant worldwide (Khan et al., 1987). In this case, the main objective was to explore temporal dynamics in plant response to salt stress. Two NaCl treatments (0 and 50 mM) were applied from three weeks after sowing until maturity, and three plants were collected for each combination cultivar × treatment at late tillering (BBCH 29), mid stem elongation (BBCH 37), flowering (BBCH 65), and maturity (BBCH 92). Cultivar Vialone Nano was not grown in this experiment given it demonstrated a response similar to Baldo at 50 mM during the first experiment. Plants were divided into stems, panicles, and apical, mid-canopy and senescent leaves. Plant height, number of tillers, dry weight of AGB and of biomass of the different organs, and Na^+ content of each organ were measured, as well as gLAI. Daily evapotranspiration was estimated by applying a gravimetric method each three days, i.e., each time the hydroponic solution was renewed. Spikelet sterility was determined at flowering and harvest.

Analysis of variance (ANOVA) was performed to evaluate the effect of salt treatment and genotype on crop response to salt stress; the Kruskal-Wallis test (Kruskal and Wallis, 1952) was used in case of violation of the assumption of normality. Statistical analysis was performed using R 3.1.0 (R core team, 2014).

2.2. The Model

The salinity model proposed by Paleari et al. (2017a) was used, coupled to the crop model WOFOST (Van Diepen et al., 1989). In particular, we used the version of WOFOST proposed by Stella et al. (2014), available at: http://www.cassandralab.com/components/1.

The parameter set for Baldo was calibrated and validated using data from the second and first experiments, respectively. For Vialone Nano, data from the 0 mM and 50 mM treatments (first experiment) were used for calibration and data from remaining treatments for validation. For Pokkali, data from the second experiment were used for calibration, whereas validation was carried out by using data from the experiment described by Yeo et al. (1986). In this case, data were collected during a growth chamber experiment with seedlings grown under four NaCl treatments (0, 25, 50, and 100 mM).

The agreement between measured and simulated values was evaluated using mean absolute error (MAE, 0 to +∞, optimum 0), root mean square error (RMSE, 0 to +∞, optimum 0), Nash and Sutcliffe modelling efficiency (EF, -∞ to 1, optimum 1), coefficient of residual mass (CRM, -∞ to +∞, optimum 0), and coefficient of determination (R^2).

Crop Sci. Accepted Paper, posted 02/15/2019. doi:10.2135/cropsci2018.10.0609

3. Results

3.1. Growth chamber experiments

A marked heterogeneity in cultivar response to salinity was observed in both experiments (Figs. 1 and 2). In the first one, salinity strongly affected growth of both Baldo and Vialone Nano at heading (Fig. 1a), with the latter showing a more linear reduction of AGB for increasing salinity levels. At the same phenological stage, larger differences between cultivars were observed for gLAI (Fig. 1b), with Vialone Nano presenting higher reduction rates. Vialone Nano also presented a higher tendency to reduce the number of tillers in salt-treated plants: the maximum reduction was 66% (compared to 45% for Baldo). No differences between cultivars were found in terms of decrease in plant height (around 45% for both cultivars).

The analysis of gas exchange traits (Table 1) revealed clear differences in reduction of transpiration rates (maximum reduction of 60% and 25% for Vialone Nano and Baldo, respectively) and, in contrast, a lower variability in terms of impact on net photosynthesis (maximum reduction of 31% and 43% for Vialone Nano and Baldo). As expected, Na^+ content in plant tissues increased according to salinity levels, especially in Baldo (Fig. 1c). Analysis of Na^+ content and concentration in different organs at heading (Figs. 1d and 1e) revealed a clear Na^+ partitioning pattern in both cultivars, with most Na^+ (more than 90% on average) stored in stems and senescent leaves. Similar dynamics were observed at maturity (data not shown), with small amounts of Na^+ stored in panicles (2.5% of total Na^+ content in Baldo and 5.6% in Vialone Nano). Considering the impact of salt stress on panicle biomass at harvest (Fig. 1f), the mean reduction for Baldo as compared to salt-free conditions was of 71%, whereas it was 51% for Vialone Nano. Baldo also showed the highest reduction (from 39% to 94%) of grain number per plant (it ranged from 10% to 69% for Vialone Nano). The reduction of grain weight was instead similar for the two cultivars, with minimum value of 1% and maximum of 21%.

For Baldo, salt treatments led to a delay in heading date that was proportional to the salinity level (from 16% at 10 mM to 32% at 50 mM). For Vialone Nano, the delay was observed only at 50 mM (17%).

Differences between cultivars were clearer in the second experiment (Fig. 2). The largest impact of salinity was observed for Baldo, for which the mean reduction (as compared to the control) of AGB and gLAI was 71% and 86%, respectively (Figs. 2a, 2b, 2c, 2d). For this cultivar, clear symptoms of salt stress were observed also at early stages (i.e., tillering). For Pokkali, the impact of salinity on plant growth and leaf area expansion was less evident (mean reduction of AGB and gLAI was 4.35% and 25.14%). Similar results were observed for panicle biomass, with reduction at 50 mM equal to 89% for Baldo and 13% for Pokkali. The pronounced tolerance of Pokkali was further demonstrated by the slight reduction of plant height (0.7%) and tiller number (7%); the corresponding values for Baldo were 27% and 62%.

Despite higher Na^+ concentrations in plant tissues (Figs. 2e, 2f) were observed for Baldo, the total amount of Na^+ taken up by the two cultivars was similar (Figs. 2g, 2h). This suggests that the differences in concentration were mainly due to the higher capability of Pokkali to maintain high growth rates even after Na^+ uptake rather than to the capability of excluding Na^+ at root level. Indeed, the lower concentrations observed for Pokkali were explained by the dilution of Na^+ in a larger amount of biomass. The sequestration of Na^+ in culms and senescent leaves discussed for the first experiment was observed also in the second (Figs. 2i, 2l). Despite Pokkali presented high Na^+ concentration in panicle (56.81 mg g^{-1}), no effect on spikelet sterility was observed, whereas in Baldo mean sterility was 23% at maturity (Na^+ concentration in panicle being 15.12 mg g^{-1}).

For Baldo, the number of days from transplanting to heading for the salt-stressed treatment was 27% larger than in the control in the first experiment, whereas a 20%-shortening in grain filling duration was observed in the second experiment. On average, the total crop cycle length for stressed plants was almost 10%-shorter. Instead, no effect of salinity on phenology was observed for Pokkali.

Crop Sci. Accepted Paper, posted 02/15/2019. doi:10.2135/cropsci2018.10.0609

Concerning the effect of salinity on plant transpiration, low values were measured for both cultivars for the 50 mM treatment. In particular, reduction in transpiration due to salinity ranged from 18% (on DVS 29) to 80% (on DVS 92) for Baldo, whereas it remained nearly constant around 50% for Pokkali.

3.2. Model evaluation

Despite the large variability observed among cultivars in terms of plant response to salinity for different Na^+ treatments, the model was overall able to reproduce time dynamics of AGB, gLAI, panicle biomass, and Na^+ concentration in plant tissues (Fig. 3).

Good agreement was found between measured and simulated aboveground and panicle biomass (Figs. 3a, 3b) for both the calibration and validation datasets, with R^2 ranging from 0.88 and 0.99 (Table 2). The average mean absolute error (MAE; 0 to +∞, optimum 0) for the calibration and validation datasets was 1.30 t ha^{-1} and 0.97 t ha^{-1} for AGB, whereas it was 0.85 t ha^{-1} and 0.52 t ha^{-1} for panicle biomass. The overall closeness of the agreement metrics calculated for the calibration and validation datasets demonstrates the robustness of the parameterization. Values of modelling efficiency (EF; −∞ to +1, optimum +1; Nash and Sutcliffe, 1970) were also satisfactory, with the exception of the negative value achieved for Pokkali during validation. This is partly explained by the limited variability of the observations retrieved from the study of Yeo et al. (1986), which led small uncertainties in simulated data to reflect in a poor value of EF. No systematic over- or under-estimation was observed, being the coefficient of residual mass (CRM; −∞ to +∞; optimum = 0; positive values indicate underestimation and *vice versa*; Loague and Green, 1991) always close to 0.

The agreement between measured and simulated gLAI was slightly less satisfactory for both the calibration and validation datasets (Fig. 3c; Table 2), with the model underestimating gLAI values for Pokkali and overestimating those for Baldo and Vialone Nano. In general, the model had the tendency to overestimate gLAI values during initial growth stages (gLAI lower than 5), and to underestimate gLAI at later stages. With the exception of the validation dataset for Baldo, EF was always largely positive, whereas average values of MAE and RMSE were 1.31 and 1.49, respectively. For gLAI, some differences in model performances during calibration and validation were found, with MAE ranging between 0.80 and 1.2 for the calibration dataset and from 1.47 to 2.45 for the validation one.

Higher uncertainty was achieved for the simulation of Na^+ concentration and Na^+ content, likely because the dynamics involved with these variables are the result of many different processes deeply interacting with each other, e.g., those involved with Na^+ uptake, partitioning, sequestration in structural (culm and leaf sheath) and senescent tissues, effect on plant growth. The values of R^2 for Na^+ concentration ranged from 0.55 to 0.96 for the calibration dataset and from 0.41 to 0.94 for the validation one. Corresponding values of MAE were between 5.92 mg g^{-1} and 9.63 mg g^{-1} for calibration and between 2.82 mg g^{-1} and 7.75 mg g^{-1} for validation. However, EF values were sometimes negative (e.g., in two out of five cases for the simulation of Na^+ concentration).

Parameter values derived for Vialone Nano, Baldo and Pokkali are shown in Appendix A, together with a description of the corresponding tolerance traits. Mean and standard deviation were derived from the values obtained for the three cultivars.

Crop Sci. Accepted Paper, posted 02/15/2019. doi:10.2135/cropsci2018.10.0609

4. Discussion

Large variability in response to salinity was observed among the rice cultivars grown during the experiments, both in terms of overall tolerance and of the underlying physiological mechanisms. For Vialone Nano, the capability of reducing Na^+ uptake at root level appeared as the primary tolerance strategy that, coupled with the sequestration of Na^+ in culm and senescent leaf tissues, allowed the plant to survive under salt stress conditions. These tolerance mechanisms were already described by other authors (Faiyue at al., 2012; Reddy et al., 2017), who observed how rice is able to control the transport of salt at root level via selective uptake and/or reducing the flow through the apoplastic pathway, as well as to accumulate toxic ions in senescent leaves and leaf sheaths to protect meristematic and photosynthetically active tissues. However, this cultivar proved to be tolerant only at low Na^+ concentrations, markedly reducing growth at salinity levels higher than 25 mM.

Baldo did not control Na^+ uptake as effectively as Vialone Nano, whereas it showed to be more capable to tolerate Na^+ concentration in tissues, in turn supporting crop growth even under salt stress conditions. This is in agreement with Formentin et al. (2018), who reported that the pre-activation of leaf tolerance mechanisms before the onset of ionic stress confers to this cultivar a certain level of salt tolerance. However, the analysis of panicle biomass data suggested that Baldo could be more susceptible to salt-induced sterility for grain yield, although further experiments are needed to confirm this finding. Salt stress on both Baldo e Vialone Nano delayed flowering stage, in agreement with what reported by Kathun and Flower (1995), who observed for cultivar IR36 a reduction of pollen viability and a lengthening of the vegetative stage for increasing Na^+ concentration in a greenhouse experiment. Given the marked impact of salt stress on phenology and its importance for the correct simulation of crop growth, further improvements of the model will focus on including the effect of Na^+ on the length of different growth stages.

Pokkali confirmed its high tolerance to salt stress thanks to an efficient antioxidant defence system, as reported by El Shabrawi et al. (2010). Indeed, this cultivar did not show specific strategies to regulate Na^+ uptake or partitioning to senescent leaf or culm tissues, being its tolerance strategy mainly related with the capability of managing high Na^+ content in active tissues while maintaining high biomass accumulation rates. This resulted in a lower Na^+ concentration in photosynthetic tissues (Na^+ diluted in a large amount of biomass), in turn demonstrating, as suggested by Platten et al (2013), how plant vigour can be a successful strategy for salt tolerance.

The heterogeneity in plant responses observed during the growth chamber experiments and the completeness in terms of both variables analysed and measuring period (from third-leaf stage to maturity) allow considering the dataset used as valuable to effectively test the model capability to reproduce the dynamics of Na^+ uptake, accumulation and impact on rice growth. According to our knowledge, this dataset represents one of the few cases where temporal dynamics of different variables in response to salt stress were observed starting from the earlier vegetative stages until maturity at different Na^+ concentration, thus giving the possibility to evaluate the effect of Na^+ on the overall plant growth and on different tolerance mechanisms.

Data from the two experiments allowed validating the model proposed by Paleari et al. (2017), given the good agreement achieved between measured and simulated data. Agreement metrics confirmed indeed the capability of the model to correctly reproduce the impact of salt stress on crop growth, especially the salt-induced decrease in AGB and panicle biomass. Further model development will focus on improving the simulation of gLAI and Na^+ content/concentration, these being the outputs characterized by the highest uncertainty with respect to observations. To reach this aim, a dedicated approach will be implemented for the impact of the osmotic component of salt stress (e.g. Ferrer-Alegre et al., 1997), which represents the rapid response to the increase in external osmotic pressure in terms of stomatal conductance, and thus it is responsible of a rapid decrease in crop growth at the onset of salt stress. This will likely allow improving gLAI simulation, which is now often overestimated during early stages. Moreover, given gLAI is one of

Crop Sci. Accepted Paper, posted 02/15/2019. doi:10.2135/cropsci2018.10.0609

the main drivers of Na^+ apoplastic uptake, reducing the uncertainty in the simulation of this variable would improve also the simulation of Na^+ content and concentration. Besides extending the model for the osmotic component of salt stress using data from new growth chamber experiments, further studies will be carried out to confirm its suitability for field conditions.

There is a need for developing new rice cultivars with higher and more stable yields across different environmental and management conditions, and simulation models can represent a powerful tool to support breeders.

We evaluated here a model recently developed to explicitly account for all salt-tolerance traits for which breeding programs are ongoing. Indeed, as reported by Roy et al. (2014), the strategies for improving salt tolerance can vary greatly according to the salinity level in the soil and to its dynamics during the season, as well as to the climatic and management conditions characterizing the context of cultivation. The explicit representation of key ecophysiological processes is thus crucial to allow the model to properly interpret the complex G × E × M interactions characterizing the underlying system. Moreover, the direct relationships between model parameters and plant tolerance traits make this model suitable for decomposing complex traits ("salt-tolerance") in simple ones, in turn allowing to explore association between traits and molecular markers (Dingkuhn et al., 2017). As an example, the parameter "Threshold leaf sodium concentration" could relate to candidate genes NHX and AVP, involved with the sequestration of Na^+ into leaf vacuoles (Munns and Tester, 2008). This will open to new opportunities for using crop models to effectively support breeding programs focusing on salt tolerance.

References

Amari, T, Ghnaya, T., Debez, A., Taamali, M., Ben Youssef, N., Lucchini, G., Sacchi, G.A., Abdelly, C., 2004. Comparative Ni tolerance and accumulation potentials between *Mesembryanthemum crystallinum* (halophyte) and *Brassica juncea*: metal accumulation, nutrient status and photosynthetic activity. J. Plant. Physiol. 171, 1634-1644. doi:10.1016/j.jplph.2014.06.020.

Aringhieri, R., 2010. The salt problem in soil: an overview. J. Environ. Qual. 5, 15-22. doi:10.6092/issn.2281-4485/3801.

Bertazzini, M., Sacchi, G.A., Forlani, G., 2018. A different tolerance to mild salt stress condition among six Italian rice genotypes does not rely on Na^+ exclusion from shoots. J. Plant Physiol. 226, 145-153. doi:10.1016/j.jplph.2018.04.011.

Casadebaig, P., Zheng, B., Chapman, S., Huth, N., Faivre, R., Chenu, K., 2016. Assessment of the potential impacts of wheat plant traits across environments by combining crop modelling and global sensitivity analysis. PLoS One. https://doi.org/10.1371/journal.pone.0146385

Cooper, M., Technow, F., Messina, C., Gho, C., Radu Totir, L., 2016. Use of crop growth models with whole-genome prediction: Application to a maize multienvironment trial. Crop. Sci. 56, 2141-2156. https://doi.org/10.2135/cropsci2015.08.0512

Dingkuhn, M., Pasco, R., Pasuquin, J.M., Damo, J., Soulié, J.C., Raboin L.M., Dusserre, J., Sow, A., Manneh, B., Shrestha, S., Balde, A., Kretzschmar, T., 2017. Crop-model assisted phenomics and genome-wide association study for climate adaptation of *indica* rice. 1 Phenology. J. Exp. Bot., Vol. 68, No. 15 pp. 4369-4388. doi:10.1093/jxb/erx249.

El-Shabrawi, H., Kumar, B., Kaul, T., Reddy, M.K., Singla-Pareek, S.L., Sopory, S.K., 2010. Redox homeostasis, antioxidant defense, and methylglyoxal detoxification as markers for salt tolerance in Pokkali rice. Protoplasma 245: 85. doi:10.1007/s00709-010-0144-6.

Crop Sci. Accepted Paper, posted 02/15/2019. doi:10.2135/cropsci2018.10.0609

Faiyue, B., Al-Azzawi, M.J., Flowers, T.J., 2012. A new screening technique for salinity resistance in rice (Oryza sativa L.) seedlings using bypass flow. Plant. Cell. Environ. 35, 1099-1108. doi:10.1111/j.1365-3040.2011.02475.x.

FAO. 2008. FAO Land and Plant Nutrition Management Service. http://www.fao.org/agb/agl/agll/spush/

FAO. 2009. How to Feed the World in 2050. http://www.fao.org/fileadmin/templates/wsfs/docs/expert_paper/How_to_Feed_the_World_in_2050.pdf

Ferrer-Alegre, F., Stöckle, C.O., 1999. A model for assessing crop response to salinity. Irrig. Sci. 19, 15-23. doi:10.1007/s002710050067.

Formentin, E., Sudiro, C., Perin, G., Riccadonna, S., Barizza, E., Baldoni, E., Lavezzo, E., Stevanato, P., Sacchi G.A., Fontana, P., Toppo, S., Morosinotto, T., Zottini, M., Lo Schiavo, F., 2018. Trascriptome and cell physiological analyses in different rice cultivars provide new insights into adaptive and salinity stress responses. Front. Plant. Sci. 9, 1-17. doi:10.3389/fpls.2018.00204.

Glenn, E.P., Brown, J.J., Blumwald, E., 1999. Salt tolerance and crop potential of halophytes. Crit. Rev. Plant. Sci.18, 227-255. doi:10.1080/07352689991309207.

Horie, T., Karahara, I., Katsuhara, M., 2012. Salinity tolerance mechanisms in glycophytes: An overview with the central focus on rice plants. Rice 5, 11. doi:10.1186/1939-8433-5-11.

Hossain, H., Rahman, M.A., Alam, M.S., Singh, R.K., 2015. Mapping of quantitative trait loci associated with reproductive-stage salt tolerance in rice. J. Agro. Crop. Sci. 201, 17-31. doi:10.1111/jac.12086.

IRRI (International Rice Research Institute), 2006. Bringing hope, improving lives: Strategic Plan 2007-2015. IRRI, Manila, Philippines. 61 pp.

Jacoby, R.P., Taylor, N.L., Millar, A.H., 2011. The role of mitochondrial respiration in salinity tolerance. Trends Plant Sci. 16, 614-623. doi:10.1016/j.tplants.2011.08.002.

Karlberg, L., Ben-Gal, A., Jansson, P.E., Shani, U., 2006. Modelling transpiration and growth in salinity stressed tomato under different climatic conditions. J. Ecol. Model. 190, 15-40. doi:10.1016/j.ecolmodel.2005.04.015.

Khan, A.A., Akbar, M., Seshu, D.V., 1987. Ethylene as an indicator of salt tolerance in rice. Crop Sci. 27: 1242-1247. doi:10.2135/cropsci1987.0011183X002700060031x.

Khatun, S., Flower, T.J., 1995. Effects of salinity on seed set in rice. Plant Cell Environ. 18, 61-67. doi.10.1111/j.1365-3040.1995.tb00544.x.

Kotula, L., Ranathunge, K., Schreiber, L., Steudle, E., 2009. Functional and chemical comparison of apolpastic barriers to radial oxygen loss in roots of rice (Oryza sativa L.) grown in aerated and deoxygenated solution. J. exp. Bot. 60, 2155-2167. doi:10.1093/jxb/erp089.

Kruskal, W.H., Wallis, W.A., 1952. Use of ranks in one-criterion variance analysis. J. Am. Stat. Assoc. 47, 583-621.

Lancashire, P.D., Bleiholder, H., Langelüddecke, P., Stauss, R., Van den Boom, T., Weber, E., Witzenberger, A., 1991. An uniform decimal code for growth stages of crops and weeds. Ann. Appl. Biol. 119, 561-601. doi:10.1111/j.1744-7348.1991.tb04895.x.

Martre, P., Quilot-Tourion, B., Luquet, D., Memmah, M.O., Chenu, K., Debaeke, P., 2015. Model-assisted phenotyping and ideotype design. Crop Physiology (second edition) Application for genetic Improvement and Agronomy, pp. 349-373. doi:10.1016/B978-0-12-417104-6.00014-5.

Munns, R., Tester, M., 2008. Mechanisms of salinity tolerance. Annu. Rev. Plant Biol. 59, 651-681. doi:10.1146/annurev.arplant.59.032607.092911.

Nash, J.E., Sutcliffe, J., 1970. River flow forecasting through conceptual models. Part I – A discussion of principles. J. Hydrol. 10, 282-290. doi.org/10.1016/0022-1694(70)90255-6.

Negrão, S., Curtois, B., Ahmadi, N., Abreu, I., Saibo, N., Oliveira, M.M., 2011. Recent updates on salinity stress in rice: from physiological to molecular responses. Plant Sci., 30, 329-377. doi:10.1080/07352689.2011.587725.

Crop Sci. Accepted Paper, posted 02/15/2019. doi:10.2135/cropsci2018.10.0609

Nocito, F.F, Lancilli, C., Dendena, B., Lucchini, G., Sacchi, G.A., 2011. Cadmium retention in rice is influenced by cadmium availability, chelation and translocation. Plant Cell Environ. 34, 994-1008. doi:10.1111/j.1365-3040.2011.02299.x.

Paleari, L., Movedi, E., Confalonieri, R., 2017a. Trait-based model development to support breeding programs. A case study for salt tolerance and rice. Sci. Rep. doi:10.1038/s41598-017-04022-y.

Paleari, L., Movedi, E., Cappelli, G., Wilson, L.T., Confalonieri, R., 2017b. Surfing parameter hyperspaces under climate change scenarios to design future rice ideotypes. Global Change Biol. 23, 4651-4662. doi:10.1111/gcb.13682.

Parent, B., Tardieu, F., 2014. Can current crop models be used in the phenotyping era for predicting the genetic variability of yield of plants subjected to drought or high temperature? J. Exp. Bot. 65, 6179-6189. doi:10.1093/jxb/eru223.

Platten, J.D., Egdane, J.A., Ismail, A.M., 2013. Salinity tolerance, Na^+ exclusion and allele mining of *HKT1;5* in *Oryza sativa* and *O. glaberrima*: Many sources, many genes, one mechanism? BMC Plant Biol. 13, 32. doi:10.1186/1471-2229-13-32.

R Core Team, 2014. R: A language and environment for statistical computing [Internet]. Vienna, Austria, R Foundation for Statistical Computing. Available at http://www.R-project.org/

Radanielson, A.M., Gaydon, D.S., Li, T., Angeles, O., Roth, C.H., 2018. Modeling salinity effect on rice growth and grin yield with ORYZA v3 and APSIM-Oryza. Eur. J. Agron. 100, 44-55. doi:10.1016/j.eja.2018.01.015.

Reddy, A., Francies, R.M., Rasool, Sk, N., Venkata, R., Reddy, P., 2014. Breeding for tolerance to stress triggered by salinity in rice. Int. J. Appl. Biol. Pharm. 5. doi:10.1016/j.rsci.2016.09.004.

Reddy, I.N.B.L., Kim, B.K., Yoon, I.S., Kim, K.H., Kwon, T.R., 2017. Salt Tolerance in Rice: Focus on Mechanisms and Approaches. Sci. Direct, Rice Sci. 24, 123-144. doi:10.1016/j.rsci.2016.09.004.

Reynolds, M.P., Ortiz-Monasterio, J.I., McNab, A., 2001. Application of Physiology in Wheat Breeding. Mexico, D.F.: CIMMYT.

Roy, S.J., Negrao, S., Tester, M., 2014. Salt resistant crop plants. Curr. Opin. Biotechnol. 26, 115-124. doi:10.1016/j.copbio.2013.12.004.

Stella, T., Frasso, N., Negrini, G., Bregaglio, S., Cappelli, G., Acutis, M., Confalonieri, R., 2014. Model simplification and development via reuse, sensitivity analysis and composition: a case study in crop modelling. Environ. Model. Softw. 59, 44-58. doi:10.1016/j.envsoft.2014.05.007.

Tao, F., Rötter, R.P., Palosuo, T., Diaz-Ambrona, C.G.H., Miniguez, M.I., Semenov, M.A., Kersebaum, k.c., Nendel, C., Cammarano, D., Hoffman, H., Ewert, F., Dambreville, A., Martre, P., Rodriguez, L., Ruiz-Ramos, M., Gaiser, T., Hohn, J., Salo, T., Ferrise, R., Bindi, M., Schulman, A.H., 2017. Designing future barley ideotypes using a crop model ensemble. Eur. J. Agron. 82, 144-162. doi:10.1016/j.eja.2016.10.012.

Van Diepen, C.A., Wolf, J., Van Keulen, H., Rappoldt, C., 1989. WOFOST: a simulation model of crop production. Soil Use Manage. 5, 17-24. doi:10.1111/j.1475-2743.1989.tb00755.x.

Yeo, A.R., Flowers, T.J., 1986. Salinity resistance in rice and a pyramiding approach to breeding varieties for saline soils. Aust. J. Plant Physiol. 13, 161-173. doi:10.1071/PP9860161.

Yin, X., Kropff, M.J., Stam, P., 1999. The role of ecophysiological models in QTLs analysis: the example of specific leaf area in barley. Nature, Heredity 82, 415-421. doi:10.1038/sj.hdy.6885030.

Crop Sci. Accepted Paper, posted 02/15/2019. doi:10.2135/cropsci2018.10.0609

Table 1. *Effect of salt treatments on transpiration rate, stomatal conductance, and net photosynthesis rate at heading (% reduction compared to the control).*

	NaCl concentration (mM)	**Relative reduction in transpiration rate (%)**	**Relative reduction in stomatal conductance (%)**	**Relative reduction in net photosynthesis rate (%)**
Baldo	10	13.49	20.50	11.08
	25	21.37	45.45	9.16
	35	14.12	19.27	19.35
	50	24.62	38.59	43.38
Vialone Nano	10	10.43	8.46	-3.15
	25	22.78	26.11	-5.48
	35	22.09	32.11	5.21
	50	61.74	71.49	30.82

Table 2. *Indices of agreement between measured and simulated values of aboveground biomass (AGB, t ha^{-1}), panicle biomass (t ha^{-1}), green leaf area index (gLAI, -), total plant Na^+ concentration (mg g^{-1}) and total plant Na^+ content (mg plant^{-1}) for Baldo, Vialone Nano and Pokkali.*

Activity	Cultivar	Variable	**MAE**	**RMSE**	**EF**	**CRM**	**R^2**
Calibration	Baldo	AGB	0.70	0.81	0.97	-0.09	0.98
		Panicle biomass	1.10	1.71	0.48	-0.25	0.96
		gLAI	1.02	1.15	0.80	-0.06	0.95
		Na^+ concentration	9.63	11.10	0.69	0.36	0.93
		Na^+ content	23.83	26.33	-5.14	0.19	0.65
	Vialone Nano	AGB	2.30	3.23	0.47	-0.16	0.88
		Panicle biomass	1.12	1.38	0.67	0.00	0.95
		gLAI	1.18	1.19	0.89	-0.26	0.99
		Na^+ concentration	8.27	13.59	0.26	-0.38	0.55
		Na^+ content	12.77	15.48	0.42	0.03	0.90
	Pokkali	AGB	0.90	1.28	0.93	-0.05	0.94
		Panicle biomass	0.33	0.36	0.62	0.10	0.91
		gLAI	1.18	0.91	0.75	0.12	0.88
		Na^+ concentration	5.92	6.34	-3.37	0.58	0.88
		Na^+ content	20.52	24.71	0.22	0.33	0.96
Validation	Baldo	AGB	1.44	2.17	0.84	-0.13	0.88
		Panicle biomass	0.78	1.17	0.87	-0.20	0.91
		gLAI	1.47	1.93	0.47	-0.07	0.87
		Na^+ concentration	7.75	14.20	-0.75	0.04	0.41
		Na^+ content	33.37	57.17	-1.21	0.54	0.33
	Vialone Nano	AGB	1.39	1.55	0.77	-0.25	0.97
		Panicle biomass	0.26	0.38	0.96	0.12	0.98
		gLAI	2.45	2.59	-3.54	-0.78	0.71
		Na^+ concentration	2.82	3.18	0.20	-0.46	0.88
		Na^+ content	22.10	22.82	-0.46	-0.73	0.94
	Pokkali	Total AGB	0.09	0.12	-3.72	0.09	0.99

Crop Sci. Accepted Paper, posted 02/15/2019. doi:10.2135/cropsci2018.10.0609

Figure captions

Figure 1. *First experiment: impact of increasing salt concentrations on Baldo (solid bars) and Vialone Nano (striped bars) at late heading (a, b, c, d, e) and maturity (f). Relative aboveground biomass (a), green leaf area index (b) and panicle biomass (f) refer to the ratio between salt-treated and control (0 mM) plants. Na^+ content (c) refers to total Na^+ in the plant. For Na^+ concentration (d) and partitioning (e) in different organs, tones from black to white refer to culms, basal leaves, mid-canopy leaves, apical leaves, and panicles. Significant differences are indicated with * and ** for p-values lower than 0.05 and 0.01, respectively, and refer to (a, b, c, and f) cultivar, (d, e) plant organ.*

Figure 2. *Second experiment: aboveground biomass (AGB), green Leaf Area Index (gLAI), Na^+ concentration, and Na^+ content at different growth stages in Baldo (left column, a, c, e, g) and Pokkali (right column, b, d, f, h) at 0 mM (black bars) and 50 mM (grey bars). Na^+ concentration in different plant organs at 50 mM is also reported (i, l; bars from black to white refer, respectively, to culms, senescent, mid-canopy and apical leaves, panicles). Significant differences are indicated with *, ** and *** for p-values lower than 0.05, 0.01 and 0.001, respectively, and refer to (a, b, c, d, e, f, g, h) salt treatment, (i,l) plant organ.*

Figure 3. *Measured and simulated values for (a) aboveground biomass, (b) biomass of panicles, (c) green leaf area index, and (d) total plant Na^+ concentration. The grey line indicates perfect agreement between measured and simulated data. Squares, triangles, and circles refer to cultivars Baldo, Vialone Nano and Pokkali, respectively.*

Crop Sci. Accepted Paper, posted 02/15/2019. doi:10.2135/cropsci2018.10.0609

Appendix A. *Plant traits involved with tolerance to salinity and corresponding model parameters for Vialone Nano, Baldo and Pokkali with means and standard deviation.*

Traits	*Parameters*	*Acronym*	*Cultivars used in growth chamber experiments*			Means	St.Dev.	Units
			Vialone Nano	Baldo	Pokkali			
Reduction of shoot Na^+ uptake	By-pass flow when the suberin content is maximum	(T1)RRBFmin	5.00	5.00	5.00	5.00	0.00	%
	Suberin Deposition Efficiency	(T1)SubDepEff	0.62	0.60	0.70	0.64	0.05	–
	Maximum Suberin Content*	(T1)SCmax	30.00	30.00	38.00	32.67	4.62	mg g^{-1}
Sequestration of Na^+ in structural tissues	Potential culm sequestration rate	(T2)PotCSeq	0.03	0.03	0.90	0.32	0.50	mg $plant^{-1}$
	Maximum culm sodium concentration	(T2)[Na^+]culmMax	22.00	25.00	25.00	24.00	1.73	mg g^{-1}
Tolerance to salt-induced sterility	Susceptibility to salt-induced sterility	(T3)SuscSt	0.00	0.00	0.00	0.00	0.00	–
	Sodium translocation factor to panicle	(T3)Na^+ToPan	0.15	0.40	1.00	0.52	0.44	–
Compartmentation of Na^+ into senescent leaves	Sodium partitioning capability to older leaves	(T4)PartCap	0.70	0.70	0.90	0.77	0.12	–
Tissue tolerance	Threshold leaf sodium concentration	(T5)ThreshL	1.00	2.00	25.00	9.33	13.58	mg g^{-1}
	Critical leaf sodium concentration	(T5)CritL	30.00	40.00	80.00	50.00	26.46	mg g^{-1}

*parameter value already adapted to field conditions (i.e., accounting for the difference between root development in hydroponic and soil conditions, Kotula et al., 2009

Crop Sci. Accepted Paper, posted 02/15/2019. doi:10.2135/cropsci2018.10.0609

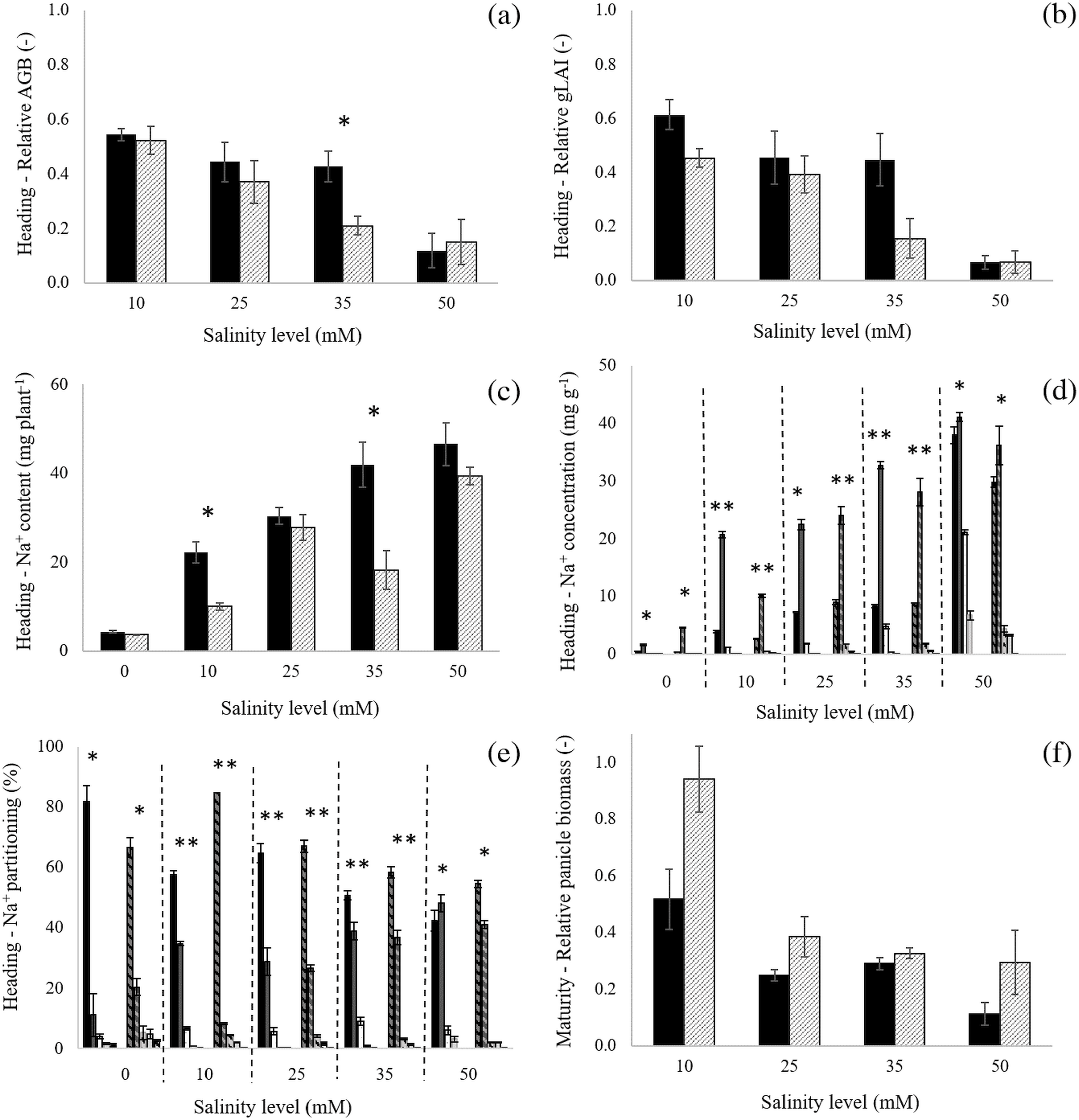

Crop Sci. Accepted Paper, posted 02/15/2019. doi:10.2135/cropsci2018.10.0609

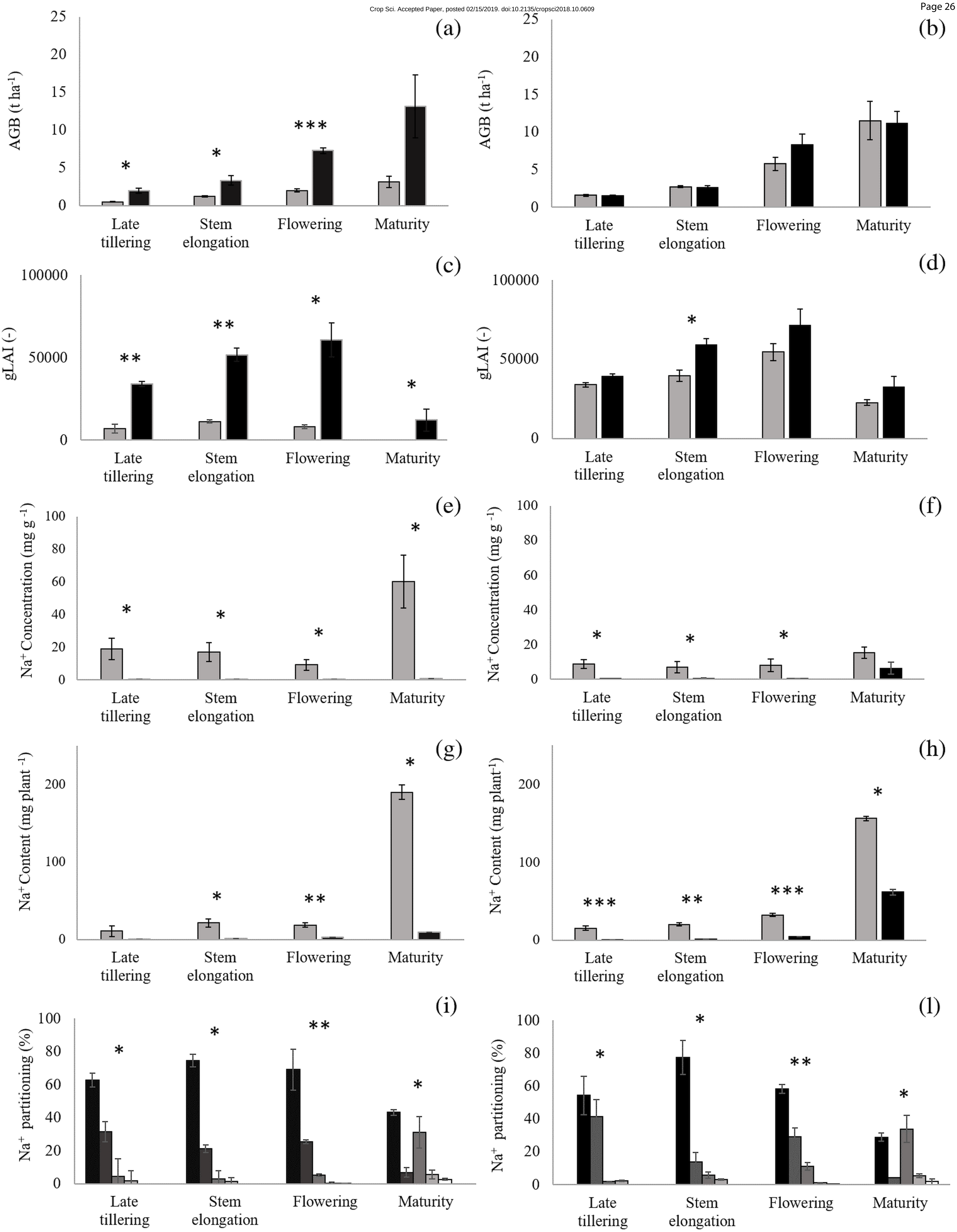

Crop Sci. Accepted Paper, posted 02/15/2019. doi:10.2135/cropsci2018.10.0609